

Facile Synthesis of Nickel Chromite Nanostructures by Hydrothermal Route for Photocatalytic Degradation of Acid Black 1 under Visible Light

Farshad Beshkar, Masoud Salavati-Niasari *

Institute of Nano Science and Nano Technology, University of Kashan, Kashan, P.O. Box 87317-51167, I. R. Iran

Article history:

Received 21/01/2015

Accepted 28/02/2015

Published online 1/03/2015

Keywords:

Nickel chromite

Hydrothermal

Photocatalytic degradation

Acid black 1

Nanostructures

*Corresponding author:

E-mail address:

salavati@kashanu.ac.ir

Phone: +98 31 55912383

Fax: +98 31 55913201

Abstract

NiCr₂O₄ normal spinel nanostructures were prepared via hydrothermal treatment at 180 °C for 12 h in the presence of cetyltrimethylammonium bromide (CTAB), sodium dodecyl sulphate (SDS) and poly vinylpyrrolidone-25000 (PVP-25000) as capping agents and subsequent calcination process at 500 °C for 3 h. In this method, [Ni(en)₂(H₂O)₂](NO₃)₂ and [Cr(en)₃]Cl₃.3H₂O used as precursors and not utilized any alkaline or precipitating agent. Detailed characterization of the as-prepared nanostructures were carried out by Fourier transform infrared (FTIR), X-ray diffraction (XRD), field emission scanning electron microscopy (FESEM), UV-Vis diffuse reflectance spectroscopy (DRS). XRD revealed the formation of pure nickel chromite spinel phase and SEM showed the formation of uniform sphere-like nanoparticles. Furthermore, the photocatalytic degradation of acid black 1 as diazo dye used in textile and dyeing water pollutants was Investigated.

2015JNS All rights reserved

1. Introduction

Spinel-type compounds with a general formula AB₂O₄ have attracted much attention because of their tremendous technological importance. In normal cubic spinel structure Fd3m, B³⁺ ions occupy octahedral sites and A²⁺ ions tetrahedral sites [1]. Chromites as a family of normal type spinel structure have many application in the fields

ranging from applied physics and material sciences to geophysics [2]. Among the transition metal chromites with spinel-type structures, NiCr₂O₄ used as a catalyst for oxidative dehydrogenation of propane [3], gas sensors [4], pigment [5], magnetic material [6] and semiconductor [7]. Since attainment of high surface area is significantly desired for mention application in above, the preparation of nanosized nickel chromite particles have engrossed notable attention and research

endeavour. The most widely used method for the synthesis of nickel chromite involves thermal treatment [8], combustion reaction [9], spray-drying [10], sol-gel combustion [11], coprecipitation [12] and hydrothermal [13]. Among these methods, hydrothermal processes have the advantages including fine crystalline oxide materials with small size distribution, controlled size and shape of particles, cost-effective and simple route [14], reproducible and high efficiency [15].

Textile pollutants such as diazo type of dyes that have two azo groups ($-N=N-$) have been considered as hazardous waste to the environment and generally are major pollutants in waste waters. These pollutants are toxic and non-biodegradable nature that threatens the health of human, animals and plants [16–17]. In the present work, we aimed to preparation of nickel chromite via surfactant-assisted hydrothermal approach in the presence of CTAB, SDS, PVP-25000 as capping agents and utilizing organometallic compounds as precursor. Following, the photocatalytic property of this nanostructure was determined to degradation of acid black 1 as a diazo type of dyes used in Textile industries.

2. Experimental procedure

2.1. Materials and characterization

Nickel chromite nanostructures, $[\text{Ni}(\text{en})_2(\text{H}_2\text{O})_2](\text{NO}_3)_2$ and $[\text{Cr}(\text{en})_3]\text{Cl}_3 \cdot 3\text{H}_2\text{O}$ were prepared, using the following chemicals, purchased from Merck Company: $\text{Ni}(\text{NO}_3)_2 \cdot 6\text{H}_2\text{O}$, ethylenediamine (en), $\text{CrCl}_3 \cdot 6\text{H}_2\text{O}$, HCl, methanol, zinc granule, cetyl trimethylammonium bromide (CTAB), sodium dodecyl sulphate (SDS), poly vinylpyrrolidone-25000 (PVP-25000), Acid black 1 (chemical formula = $\text{C}_{22}\text{H}_{14}\text{N}_6\text{Na}_2\text{O}_9\text{S}_2$, MW = $616.49 \text{ g mol}^{-1}$ and $\lambda_{\text{max}} = 618 \text{ nm}$). Powder X-ray

diffraction (XRD) patterns of products were obtained by a Philips diffractometer utilizing X'PertPro and the monochromatized Cu K α radiation ($\lambda = 1.54 \text{ \AA}$). Fourier transform infrared spectra of the samples were obtained utilizing KBr pellets on an FT-IR spectrometer (Magna-IR, 550 Nicolet) in the $400\text{--}4000 \text{ cm}^{-1}$ range. FESEM images of nickel chromite nanostructures were taken by a Tescan mira3 and Hitachi S-4160 field emission scanning electron microscopes (FESEM). The optical properties of absorption were measured by UV-Vis spectrophotometer (Shimadzu, UV-2550, Japan).

2.2. preparation of $[\text{Ni}(\text{en})_2(\text{H}_2\text{O})_2](\text{NO}_3)_2$

The complex diaquabis(ethylenediamine) nickel(II) nitrate was synthesized similar to our previous work [18]. In brief, 2 mol of ethylenediamine was added to 1 mol of $\text{Ni}(\text{NO}_3)_2 \cdot 6\text{H}_2\text{O}$ solution (in 50 ml of distilled water). The solution was stirred for about 1h then placed in an ice-bath for 1h to complete crystallization. The violet product was filtrated, washed and air-dried.

2.3. preparation of $[\text{Cr}(\text{en})_3]\text{Cl}_3 \cdot 3\text{H}_2\text{O}$

The complex tris(ethylenediamine) chromium (III) chloride trihydrate was prepared in our previous work [19]. First, 2.66 g of $\text{CrCl}_3 \cdot 6\text{H}_2\text{O}$ was dissolved in 10 mL of methanol. Then 1 g of Zn granules was added into the above solution under magnetic stirring. Next, 10 mL of ethylenediamine was added dropwise. The mixture was refluxed for 1.5h at $60 \text{ }^\circ\text{C}$. Finally, the flask was placed in an ice-bath for 1h to complete crystallization and a yellow precipitate was collected by filtration, and the granules of zinc removed. The product was washed several times with a solution including 10% of ethylenediamine in methanol and dried at room temperature.

2.4. Preparation of NiCr₂O₄ nanostructures

Nickel chromite nanostructures were synthesized hydrothermally in the presence of cationic (CTAB), anionic (SDS) and neutral (PVP-25000) surfactants. In a typical synthesis, 0.1 g of [Ni(en)₂(H₂O)₂](NO₃)₂ and 0.23 g of [Cr(en)₃]Cl₃.3H₂O were respectively dissolved in 20 ml of distilled water. Then [Cr(en)₃]Cl₃.3H₂O solution was added dropwise into [Ni(en)₂(H₂O)₂](NO₃)₂ solution under continuous magnetic stirring in room temperature. An aqueous solution (5 ml) of surfactant was added dropwise to the Cu–Cr solution mixture (molar ratio of Cu:Cr:surfactant was 1:2:0.75). After the mixture was continuously stirred for 15 min, transferred into a stainless steel autoclave of 200 ml capacity. The autoclave was sealed and maintained at 180 °C for 12 h, and then cooled to room temperature naturally. The final greenish product was washed with distilled water and absolute ethanol several times and then dried at room temperature for one day in air. After that, the as-obtained product was calcined at 500 °C for 3 h in air.

2.5. Photocatalytic test

The photocatalytic activity of as-prepared NiCr₂O₄ nanostructure (Synthesized with SDS) was evaluated by degradation of acid black 1 as diazo dye in an aqueous solution under simulative visible light at room temperature. The photocatalytic degradation was performed at neutral pH by employing 0.001 g of acid black 1 aqueous solution including 0.04 g of NiCr₂O₄ nanostructure. The suspension was sonicated for 5 min and was stirred in dark for 30 min with aeration to reaching adsorption equilibrium. A 400 W Osram lamp was used as a visible light source. At particular time intervals, 3 mL of the solution was withdrawn,

centrifuged and then were analyzed by a UV–vis spectrophotometer. The degradation percentage was calculated using the formula (1):

$$\text{Degradation (\%)} = \frac{A_0 - A_t}{A_0} \times 100$$

Where A₀ and A_t are the initial absorbance and observed absorbance of acid black 1 at 0 and t min, respectively.

3. Result and discussion

According to figure 1a-c, infrared spectrum (FT-IR) of the as synthesized [Ni(en)₂(H₂O)₂](NO₃)₂, [Cr(en)₃]Cl₃.3H₂O, and NiCr₂O₄ (Synthesized with SDS) was in the range of 400-4000 cm⁻¹ wavenumber which identify the chemical bonds as well as functional groups in the compound. FT-IR spectrum of the [Ni(en)₂(H₂O)₂](NO₃)₂ is illustrated in Fig. 1a. In this spectrum, the vibrational bands at 3223 and 3168 cm⁻¹ are corresponding to the stretching vibration of N-H of the ethylenediamine [20]. Two absorption bands at 2938 and 2884 cm⁻¹ are corresponding to the symmetry stretching and asymmetry stretching mode of the CH₂ groups of the ethylenediamine, respectively. The absorption band at 1024 cm⁻¹ can be assigned to the C–N stretching vibration. The band at 520 cm⁻¹ is related to ν(Ni–N) vibration [21]. Fig. 1b shows FT-IR spectrum of the [Cr(en)₃]Cl₃.3H₂O. Two absorption peaks at 3206 and 3042 cm⁻¹ can be assigned to the stretching vibration of N-H of the ethylenediamine. Two absorption peaks at 2939 and 2877 cm⁻¹ can be assigned to the symmetry stretching and asymmetry stretching mode of the CH₂ groups of the ethylenediamine, respectively. The absorption band at 1052 cm⁻¹ is attributable to the C–N stretching vibration. The peak at 414 cm⁻¹ is related to ν(Cr–N) vibration [22]. Fig. 1c shows FT-IR

spectrum of NiCr_2O_4 nanostructure. In this spectrum, the bands at 625 , 538 cm^{-1} are ascribed to the characteristic peaks of NiCr_2O_4 which confirms the preparation of nickel chromite [23]. The band located at 3432 cm^{-1} and the weak band at 1628 cm^{-1} are related to the $\nu(\text{OH})$ stretching and bending vibrations, respectively, which indicates the presence of water molecules linked to nickel chromite product.

X-ray diffraction (XRD) pattern was used to identify the crystalline phase and to estimate the crystalline size of nickel chromite. Fig. 2 shows the XRD pattern of samples prepared at $500\text{ }^\circ\text{C}$ for 3 h. XRD results show that the pure NiCr_2O_4 has been formed. All diffraction peaks in the XRD pattern can be readily indexed to pure cubic NiCr_2O_4 with $\text{Fd}3\text{m}$ space group (JCPDS 88-0108). The crystallite size of the NiCr_2O_4 nanostructure has been estimated from Sherrer formula according to equation the following (2):

$$D = \frac{0.89\lambda}{B \cos \theta}$$

where, 0.89 is the shape factor, λ is the x-ray wavelength, B is the line broadening at half the maximum intensity (FWHM) in radians, and θ is the Bragg angle. The crystallite size of the obtained nickel chromite from the XRD results was calculated to be about 12 nm.

Field emission scanning electron microscope (FESEM) technique was applied to investigate the effect of surfactants by using CTAB, SDS and pvp-25000 on the morphology and size of the nickel chromite. FESEM images of samples prepared in the presence of CTAB, SDS and pvp-25000 are illustrated in Fig. 3a-c, respectively. As was observed, relatively uniform sphere-like nanoparticles are formed in the presence of all three capping agents. It can be explained by LaMer theory for the crystallization nucleation- growth

process. According to this theory, the nucleation rate increases

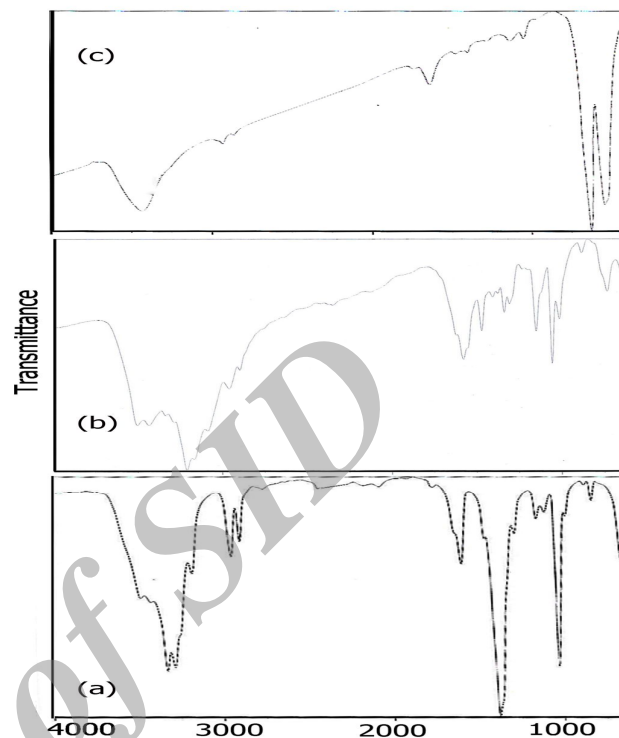


Fig. 1. FT-IR spectra of (a)- $[\text{Ni}(\text{en})_2(\text{H}_2\text{O})_2](\text{NO}_3)_2$, (b)- $[\text{Cr}(\text{en})_3]\text{Cl}_3 \cdot 3\text{H}_2\text{O}$ and (c) as-prepared NiCr_2O_4 .

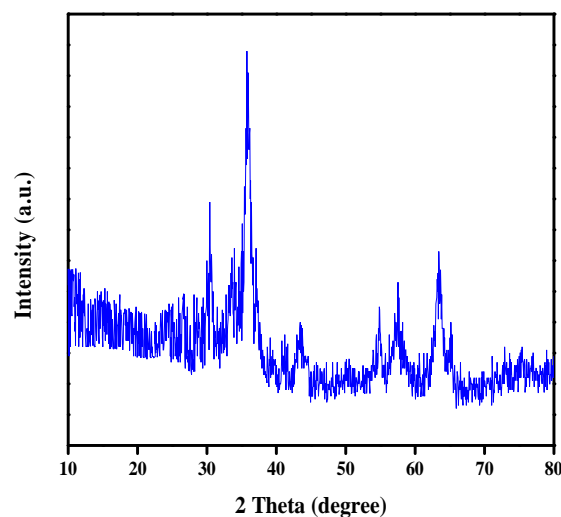


Fig. 2. XRD pattern of the products prepared at $500\text{ }^\circ\text{C}$ for 3 h.

with decreasing surface energy [24]. Here, surfactants play two roles: first, control the

nucleation rate by impressing the surface energy. Second, operate as a stabilizer to prevent aggregation of nanoparticles [25]. The SEM images demonstrates that nickel chromite nanoparticles have the average size around 60 nm.

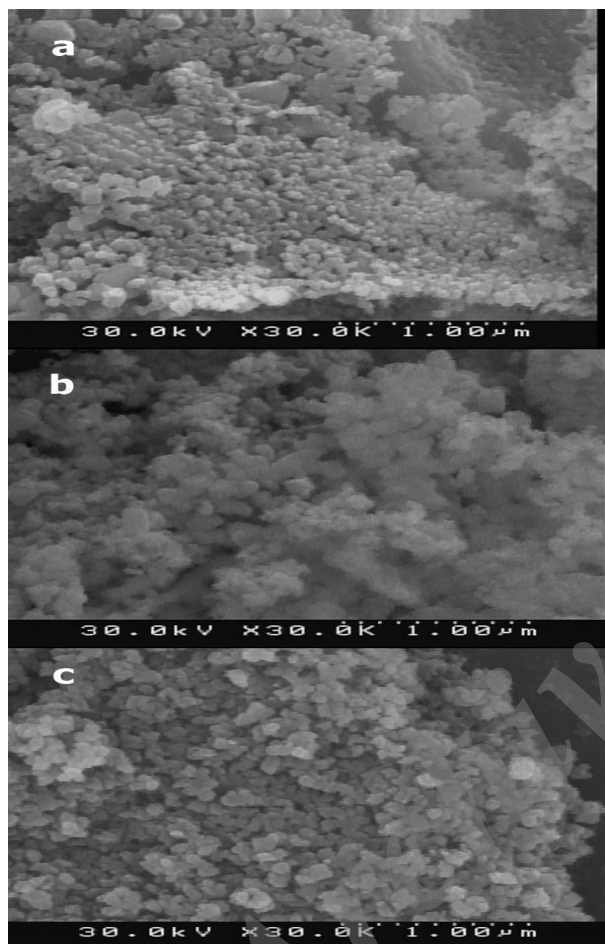


Fig. 3. FESEM images of the products prepared by hydrothermal treatment at 180 °C for 12 h in presence (a)- CTAB, (b)- SDS and (c)- PVP-25000.

Fig. 4, illustrates the UV–vis diffuse reflectance spectrum of the as-prepared NiCr₂O₄ nanostructure. As can be seen, the strong absorption band situated at low wavelength near 374 nm. The energy gap (E_g) can be calculated based on the UV–vis diffuse reflectance data by using Tauc's Equation that calculated to be 3.34 eV [26].

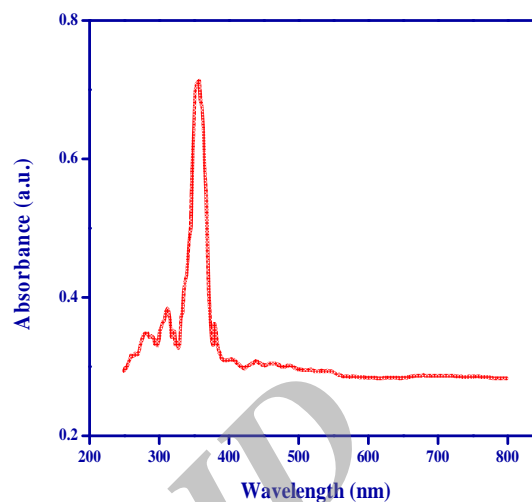


Fig. 4. UV–vis diffuse reflectance spectrum of the NiCr₂O₄ nanostructure.

To investigate the photocatalytic activity of synthesized nanoparticles, the photodegradation of the acid black 1 as diazo dye in an aqueous solution under visible light irradiation was applied. According to photodegradation calculations by Eq. (1), the acid black 1 degradation was about 75% after 120 min illumination of visible light (Fig. 5).

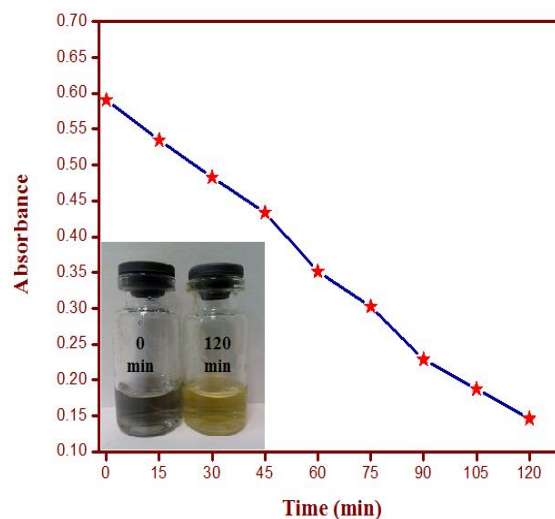


Fig. 5. Photocatalytic degradation of acid black 1 by NiCr₂O₄ nanostructure.

4. Conclusion

Briefly, nickel chromite nanostructures have been successfully prepared via a simple hydrothermal method by complexes $[\text{Ni}(\text{en})_2(\text{H}_2\text{O})_2](\text{NO}_3)_2$ and $[\text{Cr}(\text{en})_3]\text{Cl}_3 \cdot 3\text{H}_2\text{O}$ as precursors and CTAB, SDS, PVP-25000 as capping agents. This route is proved to be a simple, cost effective, dependable, environmentally friendly and efficient way. The properties of the as-prepared nanostructure characterized by the suitable analytical techniques such as FT-IR, XRD, FESEM, UV-Vis diffuse reflectance. Its photocatalytic activity was examined by degradation of diazo dye (acid black 1) in aqueous solution under visible irradiation. The percentage of diazo dye photodegradation was near 75 after 120 min that can be utilized as a candidate for photocatalytic applications.

Acknowledgment

The authors are thankful to University of Kashan for supporting this work.

References

- [1] M. Ptak, M. Maczka, A. Gagor, A. Pikul, A. Pikul, J. Hanuza, J. Solid. State. Chem. 201 (2013) 270–279.
- [2] Z. Wang, S.K. Saxena, P. Lazor, H.S.C. O'Neill, J. Phys. Chem. Solids. 64 (2003) 425–431.
- [3] J. Sloczynski, J. Ziolkowski, B. Grzybowska, R. Grabowski, D. Jachewize, K. Wcislo, L. Gengembre, J. Catal. 187 (1999) 410–418.
- [4] C.L. Honeybourne, R.K. Rasheed, J. Mater. Chem. 6 (1996) 277–283.
- [5] B.S. Barros, A.C.F.M. Costa, R.H.G.A. Kiminami, L.D. Gama, J. Metast. Nano Mater. 20–21 (2004) 325–332.
- [6] H. Ishibashi, T. Yasumi, J. Magn. Magn. Mater. 310 (2007) 610–612.
- [7] Z.Q. Hu, Y. Qin, X.Q. Liu, Adv. Mater. Res. 415–417 (2011) 1594–1598.
- [8] S.A. Bakar, N. Soltani, W.M.M. Yunus, E. Saion, A. Bahrami, Solid. State. Commun. 192 (2014) 15–19.
- [9] B.S. Barros, A.C.F.M. Costa, R.H.G.A. Kiminami, L.D. Gama, J. Metast. Nano Mater. 20–21 (2004) 325–332.
- [10] X.D. Cheng, J. Min, Z.Q. Zhu, W.P. Ye, Int. J. Miner. Metall. Mater. 19 (2012) 173–178.
- [11] G.Q. Fen, Z. Xin, G.X. Hu, Y.S. Rong, L. Gang, Chin. J. Inorg. Chem. 28 (2012) 1979–1984.
- [12] M. Ptak, M. Maczka, A. Gagor, A. Pikul, A. Pikul, J. Hanuza, J. Solid. State. Chem. 201 (2013) 270–279.
- [13] S.K. Durrani, S.Z. Hussain, K. Saeed, Y. Khan, M. Arif, N. Ahmed, Turk. J. Chem. 36 (2012) 111–120.
- [14] L.S. Wojciech, E.R. Richard, Adv. Sci, Tech. 45 (2006) 184–193.
- [15] S.S. Acharyya, S. Ghosh, R. Tiwari, B. Sarkar, R.K. Singha, C. Pendem, T. Sasaki, R. Bal, Green Chem. (2014) DOI: 10.1039/c3gc42369g.
- [16] M. Rodriguez, V. Sarria, S. Esplugas, C. Pulgarin, J. Photochem. Photobiol. A: Chem. 151 (2002) 129–135.
- [17] H. Park, W. Choi, J. Photochem. Photobiol. A: Chem. 159 (2003) 241–247.
- [18] F. Beshkar, S. Zinatloo-Ajabshir, M. Salavati-Niasari, J Mater Sci: Mater Electron. (2015) DOI 10.1007/s10854-015-3024-1.
- [19] F. Beshkar, S. Zinatloo-Ajabshir, M. Salavati-Niasari, J Mater Sci: Mater Electron. (2015) DOI 10.1007/s10854-015-3024-1.
- [20] F. Davar, M. Salavati-Niasari, Z. Fereshteh, J. Alloy. Compound. 496 (2010) 638–643.

- [21] S. Farhadi, Z. Roostaei-Zaniyani, *Polyhedron* 30 (2011) 971-975.
- [22] P.E. Aranha, M.P.D. Santos, S. Romera, E.R. Dockal, *Polyhedron* 26 (2007) 1373-1382.
- [23] Zh. Zhu, X. Cheng, W. Ye, J. Min, *Int. J. Min. Met. Mater.* 19 (2012) 266-270.
- [24] Z. Jiang, J. Xie, D. Jiang, X. Wie, M. Chen, *Cryst. Eng. Comm.* 15 (2013) 560–569.
- [25] S.S. Acharyya, S. Ghosh, R. Bal, *ACS Appl. Mater. Interfaces.* 6(16) (2014) 14451-14459.
- [26] M. Salavati-Niasari, D. Ghanbari, M.R. Loghman-Estarki, *Polyhedron* 35 (2012) 149-153.

Archive of SID